High-fidelity DEM-CFD modeling of packed bed reactors for process intensification
Proceedings of European Congress of Chemical Engineering (ECCE-6)
Copenhagen, 16-20 September 2007

High-fidelity DEM-CFD modeling of packed bed reactors for process intensification

S. Ookawara,[a] M. Kuroki,[a] D. Street,[b] K. Ogawa[a]

[a]*Department of Chemical Engineering, Tokyo Institute of Technology, 152-8552 Tokyo, Japan*
[b]*Fluent Asia Pacific, 160-0023 Tokyo, Japan*

Abstract

A high-fidelity DEM-CFD model is newly proposed for process intensification of packed bed reactors. The discrete element method (DEM) is employed for simulating random packing under gravity with hundreds of spheres in a cylindrical tube. It is verified that the DEM is capable of constituting a packed bed whose voidage well agrees with the literature according to particle-to-tube diameter ratio. The particles in or near contact are cylindrically bridged to reduce the fine and skewed computational cells around the contact point. A computational domain is then represented by connecting gaps between spherical particles each without geometrical simplification. It is shown that the pressure loss through the bed sufficiently agrees with a correlation that takes into account the particle-to-tube diameter ratio. Subsequently to the validation, the model capability for process intensification is conceptually demonstrated by specifying arbitrary boundary condition on each particle. Particles simulating inert are mixed among hot catalytic particles in laminar and random blending manners. It is confirmed that the blending style significantly affects the temperature distribution in the bed and hence it would be a design factor to be optimized by the high-fidelity DEM-CFD model.

Keywords: high-fidelity DEM-CFD model, packed bed, process intensification, sorption-enhanced reactors

1. Introduction

Blending catalytic with absorbent and/or inert particles is one of process intensifications for packed bed reactors. The former would be utilized for sorption-enhanced reactors (Xiu et al., 2003) and the latter for the control of temperature distribution and hot-spots. The laminar or random blending is a possible way to constitute such packing mixtures provided that the particle sizes are comparable (Tagawa, 2006). The mixture fraction and particle size ratio are to be locally and

globally significant factors to enhance the blending effect associated with the properties of the additive particles.

A recent high-fidelity CFD model, which represents the bed by connecting gaps between many particles each shaped without geometrical simplification, would be a potential tool to optimize these design factors. The precise reality and large scale of packing is crucial for the practical and reliable optimization. The previous hi-fi CFD models, however, typically contain only tens of spheres in a short cylinder (Nijemeisland and Dixon, 2004, Guardo et al., 2006). This is mainly due to the treatment of interparticle contact points. The particles are initially set in a tube so that they are all in contact. Subsequently, the particles are slightly made larger or smaller both to eliminate a contact point. Otherwise, infinitely fine computational cells are generated in the narrowest gap around the contact point to minimize its skewness. Even after the treatment, rather small cells are needed to fill the space between the shrunk particles or around the overlapping face edge. The necessity of such fine cells as well as adjacent small cells in bulk zone easily causes a large mesh size in total, which cannot be handled at a reasonable computational cost. The methodology is, further, essentially not tolerant about interparticle distance that could vary in random packing. Unless the particles are strictly in contact, the enlargement could generate a microscopic space that might reflexively needs a special treatment to eliminate the zone. Such restrictions certainly prevent the previous CFD models from treating a random packing with the sufficient number of particles. It should be further mentioned that the methods undesirably change the voidage compared with the initial setting. In the present study, therefore, a frame of novel numerical approach is proposed to resolve these drawbacks in the previous models.

Packed beds are modelled by allowing spherical particles to fall randomly under gravity into a cylinder. The commercial code EDEM (DEM Solutions Ltd) has been utilized for simulating the packing, which is based on discrete element method (DEM). The random packing is first examined in terms of voidage compared with the literature (Leva and Grummer, 1947), which depends on particle-to-tube diameter ratio. Subsequently, the particles in or near contact are cylindrically bridged in the stagnant region to reduce the fine computational cells around the contact point. The constituted bed is placed in a longer cylindrical tube with a same diameter for CFD analysis. The validity of the novel hi-fi DEM-CFD model is further verified regarding pressure loss through the bed, which is also much affected by the particle-to-tube diameter ratio in the examined range (Eisfeld and Schnitzlein, 2001). Modelling of particle-to-fluid heat transfer in the narrowest bed is thoroughly examined elsewhere (Kuroki et al., 2007). All the CFD procedures are performed by means of a commercial code FLUENT6.2 (Fluent Inc., 2005).

Subsequently to the validations, the laminar and random blending of catalytic and inert particles are conceptually demonstrated by specifying different boundary condition on each particle surface, which is a characteristic capability of the present hi-fi model. The influence of blending manner on the temperature distribution is examined in the bed region.

2. Numerical modeling

2.1. Particle packing by discrete element method (DEM)

In practice, a packed bed would be constituted by dumping particles into a cylindrical tube. The resultant voidage much depends upon whether the particle surface is smooth or not. It is also much affected by particle-to-tube diameter ratio. Leva and Grummer (1947) reported that the voidage of glass ball with smooth surface was sufficiently smaller than that of clay ball with rough surface at the same diameter ratio. The larger friction between rough surfaces seems to prevent the particles from being packed tightly. It was also reported that the bed voidage increased with the particle-to-tube diameter ratio regardless of the material. This might be due to the large void adjacent to the tube wall, whose contribution increases with the diameter ratio.

It is generally expected that the surface of catalytic particle is as rough as clay ball surface compared to glass ball surface. In this study, therefore, the dumping procedure is simulated by means of discrete element method to constitute the bed with a voidage of clay ball reported by Leva and Grummer (1947). The commercial code EDEM (DEM Solutions Ltd) is employed for the purpose. In the simulation, the properties of spherical particle are specified as shown in **Table 1**. The values of density, shear modulus, Poisson's ratio and coefficient of restitution are chosen referring to values of typical glass just for reality in the magnitude. It can be regarded that the coefficients of static and rolling frictions express the extent of surface roughness. However, it is beyond the scope of this study to correlate the quantified roughness with the coefficient values. The coefficient of static friction is then expediently varied to attain the desirable voidage according to the particle-to-tube diameter ratio. Since the rolling friction coefficient is usually smaller than the static friction coefficient, the value ratio is conveniently kept one hundredth in this study.

Table 1 Particle properties

properties	symbols		values
diameter	d_p	[m]	0.03
density	ρ	[kg/m^3]	2300
shear modulus	G	[Pa]	2×10^{10}
Poisson's ratio	ν	[-]	0.23
coefficient of restitution	e	[-]	0.94
coefficient of static friction	μ_s	[-]	10^{-6} – 0.2
coefficient of rolling friction	μ_r	[-]	1/100 of static friction

A cylindrical tube with same properties as particle is defined so that the axis lies in the direction of gravity. The tube height H is kept 0.6 m while the diameter D is chosen as 0.12, 0.15, 0.18, 0.21 and 0.24 m. Consequently, the particle-to-tube diameter ratio d_p/D varies from 0.125 to 0.25. A virtual cylindrical region is coaxially defined for particle generation at the tube top. The height extends 0.06 m downwards from the top and the diameter is defined as 0.75D. In this region the particles are randomly generated with an initial velocity of 0.1 m/s in the direction of gravity. The generation speed is altered according to the tube diameter so that all the particles are released in 2 s. The number of particles is varied as 220, 340, 500, 662 and 880 with an increase of tube diameter. The particles freely fall in the tube with interparticle and particle-to-tube collisions under gravity. The collisions are simulated by means of Hertz-Mindlin model (Mindlin, 1949). The velocities of all the particles are monitored and the simulation is terminated when the maximum velocity sufficiently becomes small. **Figure 1** shows a series of snapshots of the DEM simulation with the

d_p/D of 0.25. It can be seen that the dumping is well simulated by the setting described above. It is also observed that the particles are settled at 2.75 s and stable afterward. For all the diameter ratios, however, the simulations are continued at least till 5 s, which assures the maximum velocity practically becomes zero.

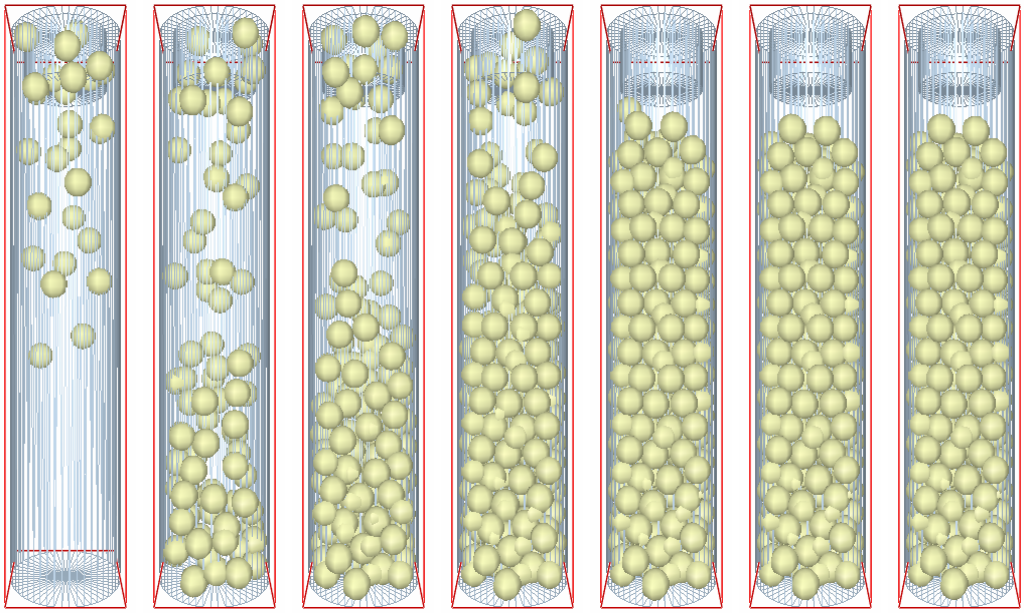

Figure 1 Snapshots of the DEM simulation with the particle-to-tube diameter ratio d_p/D of 0.25 at the time interval of 0.5 s.

2.2. Interparticle bridge model

Once the spherical particles are set in the tube by the DEM simulation, one can know the coordinates of the particle centers. Based on the coordinates and diameter, the spherical volumes are generated in a computational domain by a commercial mesh generator GAMBIT2.3 (Fluent Inc., 2006). Subsequently, the particles in or near contact are cylindrically bridged so that the cylinder axis lies on a line connecting the particle centers. The treatment to eliminate the contact zone is hereafter referred to as interparticle bridge model. The contact zone between particle and tube wall is similarly treated since the undesirable fine cells would be otherwise generated in the region. It is assumed that the bridge zone exists sufficiently within a stagnant region, which was experimentally and numerically observed near the contact in a regularly packed bed (Suekane et al., 2003; Gunjal et al., 2005). By treating all the contact zones, the particles become a giant object with the inside pores. At this stage, the object surface consists of the particle surfaces and cylinder side-walls, each of which can be separately identified.

The object is set at the middle in the circular pillar with a height of 1.5 m and with the diameter of D for the DEM simulation. A computational domain for CFD analysis is created by subtracting the volume of connected spheres from the volume of pillar. The rest of volume becomes a fluid zone in the CFD analysis, which is composed of the pores, viz., fluid paths in the bed, and empty sections at the upstream and downstream. The surface of each particle, side wall of each cylinder and tube wall still can be recognized as the independent boundaries in the CFD domain. Therefore, it is possible to specify arbitrary condition on each of these boundaries as described in

the following section. Although it is further feasible to define the solid domains inside the particles and bridging cylinders, it would be of future interest to consider the thermal conduction inside the solids.

In this study, the surface mesh is first generated on the side-wall of the cylinders. The particle surface is subsequently covered by triangular cells. The volume mesh is generated from these surface meshes. Therefore, the mesh size of the cylinder side-wall controls the total mesh size for the whole reactor. The influence of mesh size on the prediction accuracy is examined in terms of the pressure loss through the bed.

Figure 2 shows a part of geometry constituted by the interparticle bridge model and the surface mesh generated on the particle and cylinder side-wall. The particles in or near contact are bridged as seen in a solid circle. On the other hand, the distant particles, which could exist due to the random packing, are not bridged as indicated by a dotted circle. If the distance between particle surfaces is comparable to the cylinder height, in this study, the particles are not bridged. The cylinder diameter is determined so that the cylinder height sufficiently becomes large not to generate the fine cells. The effect of the cylinder diameter and the threshold of particle distance on the flow will be examined in the further study. A cylinder in a square is the bridge between particle and tube wall.

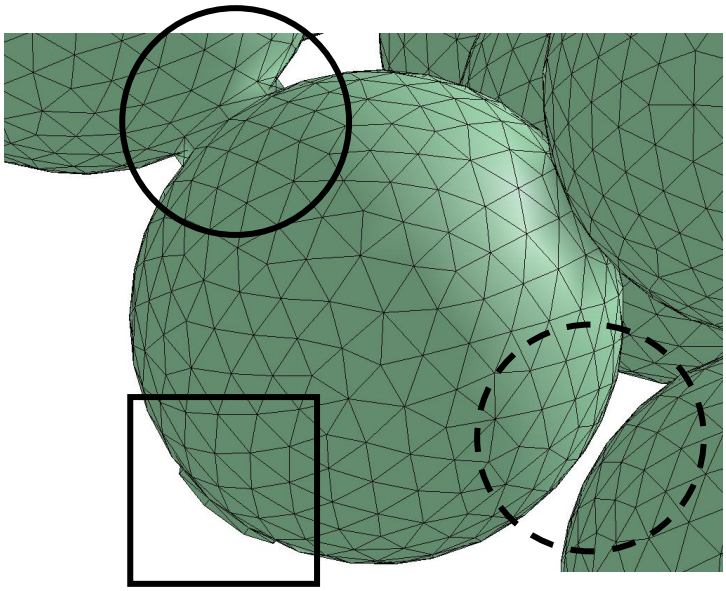

Figure 2 Geometry constituted by the interparticle bridge model and the surface mesh generated on the particle and cylinder side-wall.

2.3. CFD procedures

In this study, all the CFD procedures are performed by means of a commercial code FLUENT6 (Fluent Inc., 2005), which is based on a finite volume method. A uniform inlet velocity is defined as an inlet boundary condition. The no-slip boundary conditions are specified on the particle and cylinder surfaces as well as on the tube wall. Provided that the cylinder surface is sufficiently within the stagnant region, it can be reasonably expected that the no-slip condition does not affect the flow in the rest of volume. The effect of the interparticle bridge model on the flow is also to be examined in terms of pressure loss through the bed in this study. For the purpose,

water is chosen as a test fluid, whose density and viscosity is 1000 kg/m^3 and 0.001 Pa-s, respectively.

On the other hand, air is selected as a test fluid to demonstrate the model capability for the process intensification. As the boundary conditions of the air, a uniform velocity and temperature of 300 K is specified at the inlet. In this case, the tube wall is also specified as 300 K. The particle surface is differently specified according to assumed blending manner. In the first case, all the particle surfaces are specified as 400 K, as all the particles are catalytic and hence hot due to the reaction. In the following two cases, zero heat-flux through the surface is specified on approximately half of the particles, which can be regarded as inert. The laminar and random blending manner is demonstrated by specifying these catalytic and inert boundary conditions on corresponding particles as shown in **Figure 3**. In the laminar blending, hot particles constitute 3 layers at the middle and at the both ends of the bed while there exist two inert particle layers between the catalytic layers. Each layer contains 44 particles and therefore 132 of 220 particles are specified as the catalytic hot particles in the whole bed. On the other hand, in the random blending, 110 of 220 particles are specified as the hot particles and the rest particles are specified as the inert.

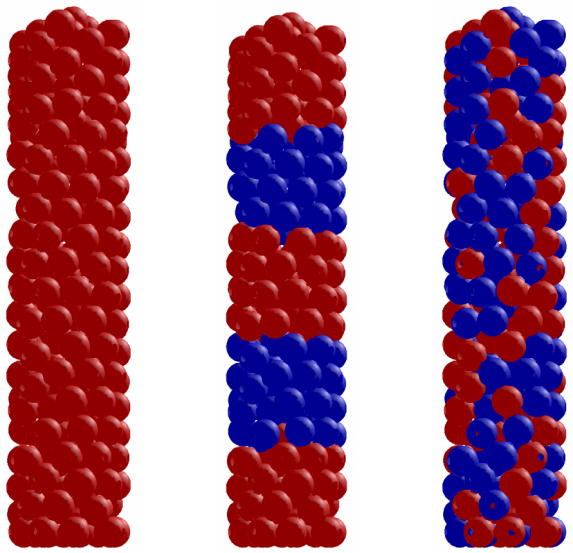

(a) (b) (c)

Figure 3 Examined configurations of hot catalytic particles with 400 K shown in red and inert particles with zero heat-flux shown in blue. (a) all catalytic, (b) laminar blend, (c) random blend. (d_p/D = 0.25)

3. Results and discussion

3.1. Voidage

Figure 4 shows the constituted beds in the d_p/D range of 0.125 to 0.25. Although the number of particles is determined so that the bed height becomes nearly same regardless of the tube diameter, the resultant bed height decreases with the tube diameter. This is partially because the contribution of large void near tube wall becomes small in the wide tube. Accordingly, it seems that the randomness of particle arrangement decreases with the tube diameter.

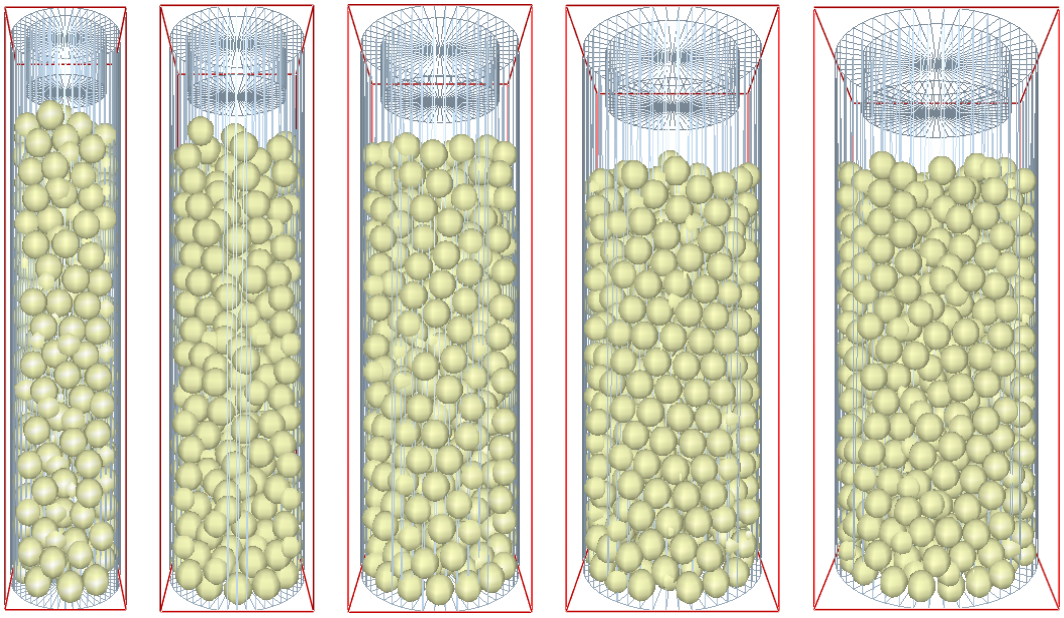

Figure 4 Random packing of spherical particles constituted by DEM simulations in the d_p/D range of 0.125 to 0.25.

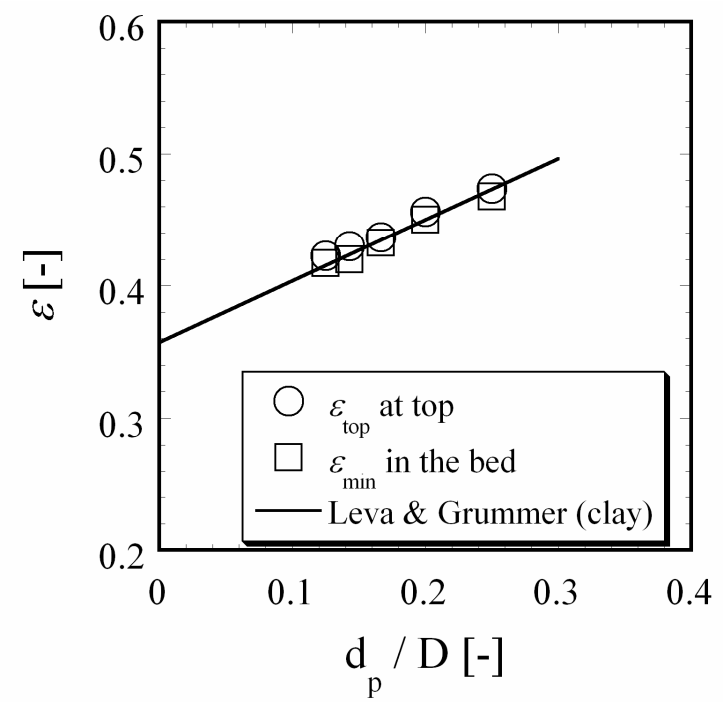

Figure 5 Comparison of voidage predicted by DEM simulation with the literature.

The voidage is evaluated for each particle in the bed based on the number of particles existing under the particle and the distance from the bed bottom. The minimum voidage ε_{min} is found near the top and the voidage at the top ε_{top} is sufficiently higher than ε_{min} due to the coarse packing at the bed top. **Figure 5** shows the comparison of the voidage predicted by the DEM simulation with the work of Leve and Grummer using the clay ball (1947). It can be seen that the predicted voidage well agrees with

the literature, which is actually due to the adjustment of the static friction coefficient. The values to attain the agreements are listed in **Table 2**. Although it is desirable that the coefficient is a constant as one of material properties, the smaller coefficient is needed to attain the proper voidage in the wider tube. On the other hand, the smaller coefficient causes an undesirable low voidage in the narrow tube. It should be still noted, however, that the DEM simulation is capable of constituting the random packing with appropriate voidage according to the particle-to-tube diameter ratio. The numerical conditions of the DEM simulation should be further examined in future for the appropriate packing with a constant friction coefficient.

Table 2 Static friction coefficients to attain the appropriate voidage.

diameter ratio d_p/D	static friction coefficient μ_s
0.250	0.150
0.200	0.100
0.167	0.015
0.143	10^{-5}
0.125	10^{-6}

3.2. Pressure loss

As shown in **Figure 6**, the pressure loss predicted by CFD is compared with a widely accepted Ergun equation (a solid line) and a recently proposed Eisfeld-Schnitzlein equation (colored dotted lines), which takes into account the particle-to-tube diameter ratio (2001). As the diameter ratio d_p/D increases, viz., the tube becomes narrower compared to the particle diamater, the E-S equation gives the pressure loss significantly higher than the Ergun equation in the lower Reynolds number range. To the contrary, the E-S equation gives slightly lower pressure loss compared to Ergun equation in the higher Reynolds number range.

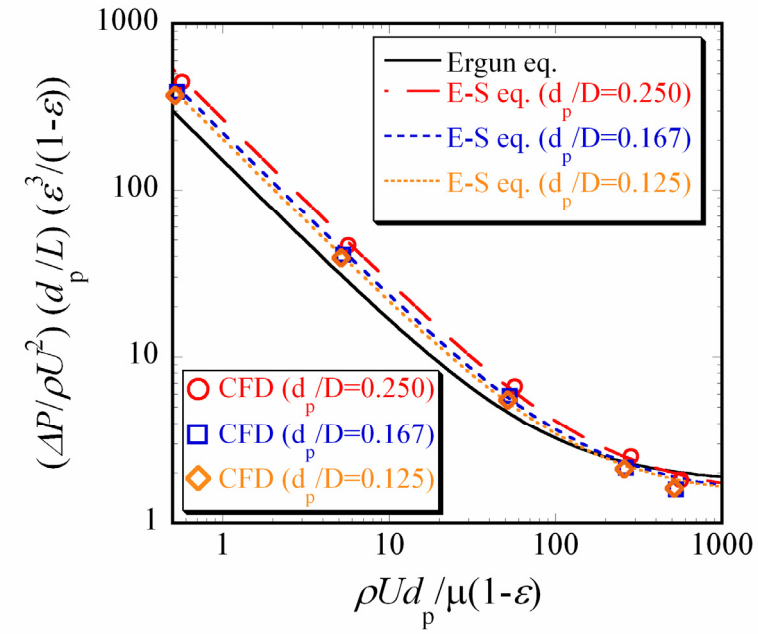

Figure 6 Pressure loss predicted by CFD with interparticle bridge model and the correlations proposed by Ergun (a solid line) and Eisfeld-Schnitzlein (colored dotted lines).

Ergun equation:

$$\left(\frac{\Delta P}{\rho U^2}\right)\left(\frac{d_\mathrm{p}}{\mathrm{L}}\right)\left(\frac{\varepsilon^3}{1-\varepsilon}\right)=150\left(\frac{1-\varepsilon}{\rho U d_\mathrm{p}/\mu}\right)+\frac{7}{4} \tag{1}$$

Eisfeld-Schnitzlein equation:

$$\left(\frac{\Delta P}{\rho U^2}\right)\left(\frac{d_\mathrm{p}}{L}\right)\left(\frac{\varepsilon^3}{1-\varepsilon}\right)=K_1 {A_\mathrm{w}}^2\left(\frac{1-\varepsilon}{\rho U d_\mathrm{p}/\mu}\right)+\frac{A_\mathrm{w}}{B_\mathrm{w}} \tag{2}$$

$$A_\mathrm{w}=1+\frac{2}{3\left(D/d_\mathrm{p}\right)(1-\varepsilon)} \qquad B_\mathrm{w}=\left[k_1\left(\frac{d_\mathrm{p}}{D}\right)^2+k_2\right]^2 \tag{3}$$

For spherical particles, the values of K_1, k_1 and k_2 are given as 154, 1.15 and 0.87, respectively.

It can be seen that the CFD-predicted pressure loss well agrees with the E-S equation rather than Ergun equation. Therefore, it is reasonable that the interparticle bridge model does not affect the macroscopic flow properties such as the pressure loss probably due to the stagnant region existing even outside of the cylinder in practice. In addition, the validity of the interparticle bridge model is thoroughly examined in terms of particle-to-fluid heat transfer somewhere else (Kuroki et al., 2007). Based on the study, it is noted that the mesh density given in this study gives an accurate heat transfer coefficient at the examined Reynolds number in the following section.

3.3. Blending manner and temperature distribution

Figure 7 shows the temperature distributions over the cross section in the narrowest bed affected by the blending manner of hot catalytic and inert particles. Because of the random packing, the size of particle cross-section varies over the plane. When all the particles are specified as 400 K, the air temperature reaches nearly maximum, viz., 400 K in the bulk zone at the middle of the bed except near the tube wall with 300 K, as seen in Fig. 7(a). In this case, the sufficient heat transfer cannot be expected at the downstream. The resultant heat transfer per particle becomes as small as 2.48 W over the whole bed. In the laminar blending bed of Fig. 7 (b), on the other hand, the air temperature repeatedly rises in the hot particle layers while the hot streams are dispersed in the inert zones. It can be seen that the low temperature zone develops along the tube wall in the inert layers due to the heat removal through the wall. The flattened temperature profile obtained in the inert is likely to decrease the particle that does not contribute to the heat transfer in the subsequent hot layer. Consequently, the heat transfer per hot particle reaches 3.44 W over the three hot layers. Through the bed of random blending shown in Fig. 7 (c), the air temperature rises gradually and it does not reach the maximum at the downstream end. This is simply because the hot particles are diluted by the inert particles. The resultant heat transfer per hot particle is as highest as 3.67 W.

Since the laminar blending bed contains 132 hot particles while there exist only 110 of hot particles in the random blending bed, the comparison in terms of heat transfer per particle might not be reasonable in case. In spite the heat transfer per particle is smaller, the total heat transfer from all the hot particles in the laminar blending bed is larger than in the random blending bed. Therefore, it would be of further interest to compare the blending manners with the same number of hot particles. It can be immediately understood that this kind of comparison might be very useful provided that the reaction rate is considered instead of heat transfer. The additive particles

might be inert, absorbent or mixture of them. The accurate modelling of catalytic particle with reactions as well as a variety of additive particles is crucial for attaining CFD-aided process intensification of packed bed reactors. The transport of chemical species can be usually treated in a commercial CFD code. Then, the particle modelling aforementioned will be hopefully realized by a user subroutine, in which the code mostly allows one to define the models of reaction and adsorption on the particle boundary surface.

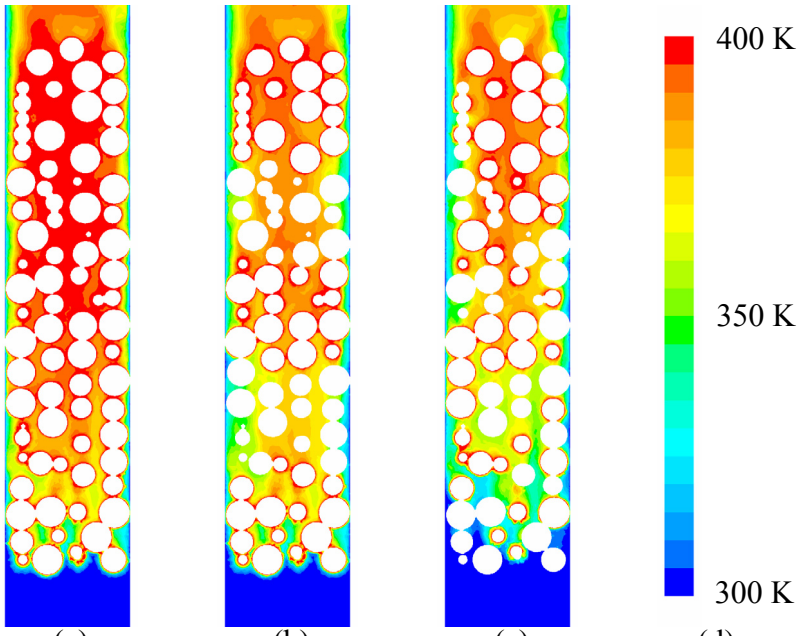

Figure 7 The influence of blending manner of hot catalytic and inert particles on the temperature distribution in the bed. (a) all catalytic, (b) laminar blend, (c) random blend, (d) colour bar for temperature distribution. ($\rho U d_p/\mu = 510$)

4. Conclusions

The present study describes the novel numerical approach for the process intensification of packed bed reactors. The DEM simulation is utilized to constitute a random packing with an appropriate voidage according to particle-to-tube diameter ratio. The interparticle bridge model is introduced to eliminate fine cells around the contact zone between particles for the CFD analysis. The assumption that the bridging cylinder exist in the stagnant region is validated in terms of pressure loss through the bed. The model capability for the process intensification is demonstrated by examining the effect of blending manner of hot and inert particles on the temperature distribution. For the practical and reliable utilization, in future, mass transfer and surface reaction should be incorporated into the model, which is currently being under progress. By developing a numerical model of absorbent particle, further, it is expected that the sorption-enhanced reactor will be rationally optimized by means of the novel DEM-CFD approach associated with the interparticle bridge model.

Acknowledgments

This research was partially supported by Asano Scholarship Foundation for Chemical Engineering.

References

Eisfeld, B. and Schnitzlein, K., (2001) *Chemical Engineering Science*, 56, 4321-4329.

Fluent Inc., (2005) *FLUENT 6.2 User's Guide*.

Fluent Inc., (2006) *GAMBIT 2.3 User's Guide*.

Guardo, A., Coussirat, M., Recasens, F., Larrayoz, M. A. and Escaler, X., (2006) *Chemical Engineering Science*, 61, 4341-4353.

Gunjal, P. R., Ranade V. V. and Chaudhari, R. V., (2005) *AIChE Journal*, 51, 365-378.

Kuroki, M., Ookawara, S., Street, D. and Ogawa, K., (2007) ECCE-6, Copenhagen, 16-21 September, 2007.

Leva, M. and Grummer, M., (1947) *Chemical Engineering Progress*, 43, 713-718.

Mindlin, R. D., (1949) *Journal of Applied Mechanics*, 16, 259-268.

Nijemeisland, M. and Dixon A. G., (2004) *AIChE Journal*, 50, 906-921.

Suekane, T., Yokouchi, Y. and Hirai, S., (2003) *AIChE Journal*, 49, 10-17.

Tagawa, T., (2006) *Chemical Engineering of Japan*, 70, 286-289. (Japanese)

Xiu, G., Li, P. and Rodrigues, A. E., (2003) *Chemical Engineerig Science*, 58, 3425-3437.